

## Study the effects of MgO nanoparticle addition on superconducting characteristics of $\text{Bi}_{1.6}\text{Ag}_{0.4}\text{Sr}_{1.9}\text{Ba}_{0.1}\text{Ca}_2\text{Cu}_3\text{O}_{10+\delta}$ system

A. S. Baqi<sup>a</sup>, N. S. Abed<sup>b\*</sup>, S. J. Fathi<sup>a</sup>

<sup>a</sup> College of science, University of Kirkuk, Iraq

<sup>b</sup> Directorate of Education of Kirkuk, Kirkuk, Iraq

In the present work, impacts adding magnesium oxide (MgO) powders with a mean particle size <100nm to Bi2223 superconducting system have been researched. The bulk samples with a general  $\text{Bi}_{1.6}\text{Ag}_{0.4}\text{Sr}_{1.9}\text{Ba}_{0.1}\text{Ca}_2\text{Cu}_3\text{O}_{10+\delta} + (\text{MgO})_x$  nominal composition formula ( $x = 0, 0.1, 0.2,$  and  $0.3\text{wt}\%$ ) have been made through the traditional solid state reaction approach. Hole concentration ( $p$ ) and Critical temperature ( $T_c$ ) of the nano MgO added samples have been specified through 4 probe techniques. X-ray powder diffraction (XRD) measurement has been utilized for examining the formation of the phase, lattice parameters and volume fraction. The results of the XRD had shown that lattice parameters are changed with the increase of the addition of the nano Mg. It has been observed as well from the measurements of the XRD that volume fraction of Bi2223 phase is increased with the increase in the addition of the nano Mg. Bi2223 phase volume fraction for non-added sample had shown that the maximum value as 77% and additionally increasing the nano MgO, Bi2223 phase's volume fraction is increased with the increase in the Bi2212 phase. The sample with addition of 0.3wt% MgO had shown the maximum Bi2223 phase volume fraction (about 80%) and maximum super-conducting transition temperature,  $T_c$  (up to 141K) in comparison with added samples with the nano MgO.

(Received January 8, 2022; Accepted April 20, 2022)

**Keywords:** (Bi-2223) superconductor, Structural properties, Critical temperature, Magnesium oxide

### 1. Introduction

Since discovering the high temperature super-conductors (HTSC), several researches were carried out in Bi2223 systems for the purpose of understanding the physical, structural, and mechanical characteristics. Substitutions or additions in Bi2223 system could result in changes in the oxygen amounts, grain orientations, and crystal structures, considerably affecting the  $J_c$  values of the Bi2223 ceramics [1-3]. Doping researches had shown that substituting or adding micro and nano-size dopants is one of the sufficient methods for the improvement of flux pinning capability and intergrain connectivity in the Bi2223. Lately, effects of the nano addition was investigated in detail, for the purpose of improving super-conducting characteristics, like the nano elements (Au, Ag, and so on), the nano oxides (ZrO<sub>2</sub>, SnO<sub>2</sub>, MgO, and so on) [4-7]. In the case where the NPs have been added to Bi2223 system, they are capable of settling easier amongst grains of those super-conductors as a result of small NP sizes. In addition to that, adding the NPs (10nm–60nm) to high temperature super-conductors has a significant impact on the enhancement of flux pinning and critical current density [8, 9]. However, substituting the NPs has resulted in the significant enhancement of inter-granular interactions. Nanosized addition for the Bi2223 system, etc. MgO [10], Al<sub>2</sub>O<sub>3</sub>[11], ZnO [12], Eu<sub>2</sub>O<sub>3</sub> [13], SnO<sub>2</sub>[14], NiFe<sub>2</sub>O<sub>4</sub>[15] and Fe<sub>2</sub>O<sub>3</sub>[16] were stated as showing the enhancement in transport characteristics. In several of the researches, the effects of the additions of the nanosize particles on the Bi2223 system were researched. Yaheya *et al.* [10] had stated effects of various nano-size magnesium oxide on transporting Bi2223 phase's critical current density. In this research, it has been found that the volume fraction increases considerably by adding 20nm of the MgO in comparison with the pure sample and addition of 40nm magnesium oxide and high volume fraction have been obtained for the sample with  $x = 0.15\text{wt}\%$ . Suazilina

\* Corresponding author: noor1988saad@gmail.com

<https://doi.org/10.15251/JOR.2022.182.273>

*etal.* [17] had stated the effect of adding Y<sub>2</sub>O<sub>3</sub> NPs in the Bi<sub>2</sub>212 super-conductors. It has been discovered that critical current density and critical temperature were increased up to  $x = 0.7\text{wt}\%$ . Zelati *etal.* [18] had explained effects of adding Dy<sub>2</sub>O<sub>3</sub> NPs on the superconducting and structural characteristics of the Bi<sub>2</sub>223 system. Based on their results, the optimal inter-grain connectivity, the maximum concentration of the hole and optimal measurements of the ac susceptibility have been obtained for the sample with  $x = 0.5\text{wt}\%$  and the onset of T<sub>c</sub> has been noticed at 109.5K. Zouaui *etal.* [19] Investigated effects of adding nano-sized ZrO<sub>2</sub> on flux pinning characteristics of the (Bi–Pb)-2223 super-conductor. The critical current density J<sub>c</sub> behaviors in the applied magnetic field and volume pinning force density F<sub>p</sub> have been improved with adding 0.1wt% ZrO<sub>2</sub>, based on their research. Saad *etal.* [20] had investigated characterization and synthesis of adding Ag NPs on Bi<sub>2</sub>223 super-conducting thin films. It has been discovered that maximum volume fraction 66.15% of Bi<sub>2</sub>223 phase and the optimal critical temperature 103.5K in comparison with other samples. Which is why, volume fraction and T<sub>c</sub> have been enhanced by the increase of the Ag NPs to 1wt%.

Zelati *etal.* [13] had stated impacts of adding Eu<sub>2</sub>O<sub>3</sub> NPs on the superconducting and structural characteristics of the Bi<sub>2</sub>223 system. Results have shown that adding Eu NPs of a sample with  $x = 0.5\text{wt}\%$  enhanced super-conducting characteristics, like the critical current density and inter-grain connectivity. Those researches have shown that a variety of the NP additions have resulted in increasing critical temperature (T<sub>c</sub>) and inter-grain connectivity, leading to improving the super-conducting characteristics of the Bi<sub>2</sub>223 system. With the developments of the nanotechnology, many different nano-structure materials were synthesized [13]. In nano-size range, particles have high rate of the atoms that have been located at the surface in comparison with the bulk materials, which has given rise to distinctive chemical and physical characteristics which are quite different from the bulk counterparts [21]. The Nano-sized addition to the Bi<sub>2</sub>223 system had resulted in the enhancement of the connectivity between grains as a result of the small sizes [13]. However, nano-sized particles had shed light on inter-grain weak links concerning the inter-granular critical current [22]. In addition to that, numerous efforts that are related to the addition or doping of the NPs were carried out on improvements of the magnetic and physical characteristics of the Bi<sub>2</sub>223 system. It can be evident from those studies that values of the J<sub>c</sub> are affected positively in the case where different nano-size particles like the SiC, ZrO<sub>2</sub>, Al<sub>2</sub>O<sub>3</sub> and MgO into high temperature superconductors enter the structure of the BSCCO [22, 23]. In earlier studies, the impacts of the super-conducting parameters of the addition of the nano-SnO<sub>2</sub> on Bi<sub>2</sub>223 system and effects of adding Nb<sub>2</sub>O<sub>5</sub> on the super-conducting characteristics of Bi<sub>2</sub>223 system have been stated [14, 24]. In addition to that, Kocabass *etal.* [25] had researched effects of substituting the micro-size Mg in Bi<sub>2</sub>223 super-conductor and maximum critical temperature has been reported as 112K up to 0.1 content.

In the present study, samples with various concentrations of nano-MgO ( $x = 0\text{--}0.3\text{wt}\%$ ) have been produced with the use of the traditional solid state approach of the reaction and effects of nano-MgO particles on the superconducting and structural characteristics of the Bi<sub>1.6</sub>Ag<sub>0.4</sub>Sr<sub>1.9</sub>Ba<sub>0.1</sub>Ca<sub>2</sub>Cu<sub>3</sub>O<sub>10+ $\delta$</sub>  super-conductor ceramics have been researched.

## 2. Experimental details

Super-conducting sample with the nominal composition Bi<sub>1.6</sub>Ag<sub>0.4</sub>Sr<sub>1.9</sub>Ba<sub>0.1</sub>Ca<sub>2</sub>Cu<sub>3</sub>O<sub>10+ $\delta$</sub>  have been produced from the approach of the solid state reaction, as suggested by N. S. Abed et al. [26]. Superconducting samples with the nominal composition Bi<sub>1.6</sub>Ag<sub>0.4</sub>Sr<sub>1.9</sub>Ba<sub>0.1</sub>Ca<sub>2</sub>Cu<sub>3</sub>O<sub>10+ $\delta$</sub>  + (MgO)<sub>x</sub> where ( $x = 0.00, 0.1, 0.2, \text{ and } 0.3\text{wt}\%$ ) have been produced by the approach of the solid state reaction, with the use of the Starting materials have been AgO (Merck > 99%), (Bi<sub>2</sub>O<sub>3</sub> (Aldrich > 99:9%), BaO (Merck > 99%), SrCO<sub>3</sub> (Diopma >99:99%), CuO (Diopma > 99:99%), CaCO<sub>3</sub> (Diopma < 99:99%), and MgO nano with a high purity of approximately 99.99%. samples have been respectively labeled as Mg0 ( $x = 0.0\text{wt}\%$ ), Mg1 ( $x = 0.1\text{wt}\%$ ), Mg2 ( $x = 0.2\text{wt}\%$ ), and Mg3 ( $x = 0.3\text{wt}\%$ ). They have been calcined at 120°C for 1.5h and after that powder mix has been calcined again at 800°C for 15h with the intermediate grinding. Calcined samples have been ground once more and pressed into the pellets of 13.0mm diameter and about 1.5mm thick at a

pressure of 7ton/cm<sup>2</sup> using a pressing machine. Ultimately, those pellets have been sintered at 850°C for 140h at a (5°C/min) heating rate, cooled down after that to the temperature of the room in the air. The schedule of the heat treatment for the Bi2223 pellets in the programmable temperature controlled silicon carbide (SiC) furnace. The structural features of 2223-phase has been checked with the use of the XRD method with the use of the (Shimadzu XRD6000) diffractometer with the source Cu-K $\alpha$  (1.5406Å) radiation in range of the diffraction angle of (20° – 60°). Lattice parameters a, b and c have been estimated with the use of d-values and (hkl) reflection of observed XRD with the use of the standard card (ICDD042-0743) for the Bi2223, and (ICDD079-2183) for the Bi2212. Volume fraction for any phase that has been determined with the use of the equation:

$$V_{ph} = \frac{\sum I^o}{\sum I^o + \sum I_1 + \sum I_2 + \sum I_n} \times 100\% \quad (1)$$

where  $I^o$  represents peak intensity of XRD of a phase that has been determined,  $I_1$ ,  $I_2$  and  $I_n$  represent peak intensities of all XRD. Mass density ( $dm$ ) can be calculated from the following formula:

$$dm(gm\ cm^3) = \frac{Mwt}{NA \times V} \quad (2)$$

$NA$  represents the avogadro number ( $6.022 \times 10^{23} mol^{-1}$ ),  $V$  represents unit cell volume and  $Mwt$  represents molecular weight.

Oxygen content has been determined with the use of chemical approach that has been referred to as the iodometric titration has been explained elsewhere [27]. A four probe method has been utilized for the measurement of electrical resistivity as function of the temperature at temperature range of (100K-300K) by using equation:

$$\rho = \frac{(R \times A)}{L} \quad (3)$$

### 3. Results and discussion

#### 3.1. XRD Results

Figure1 illustrates the patterns of the XRD of all of the samples, showing orthorhombic poly-crystalline structure for all of the samples which were composed throughout the synthesis of the samples and noticed that all samples include a high ratio of high temperature phase (Bi2223) and a few low temperature phase peaks (Bi2212) and that has low temperature, with the appearance of a few of the phases with unknown impurity that have been in agreement with [28]. The appearance of over 2 phases might be associated with stacking faults along c-axis or/and a result of substituting the MgO that result in the deformation of structure. It is observed that increasing the concentration of Mg results in causing an increase in the peak intensity, as can be seen from Figures1.

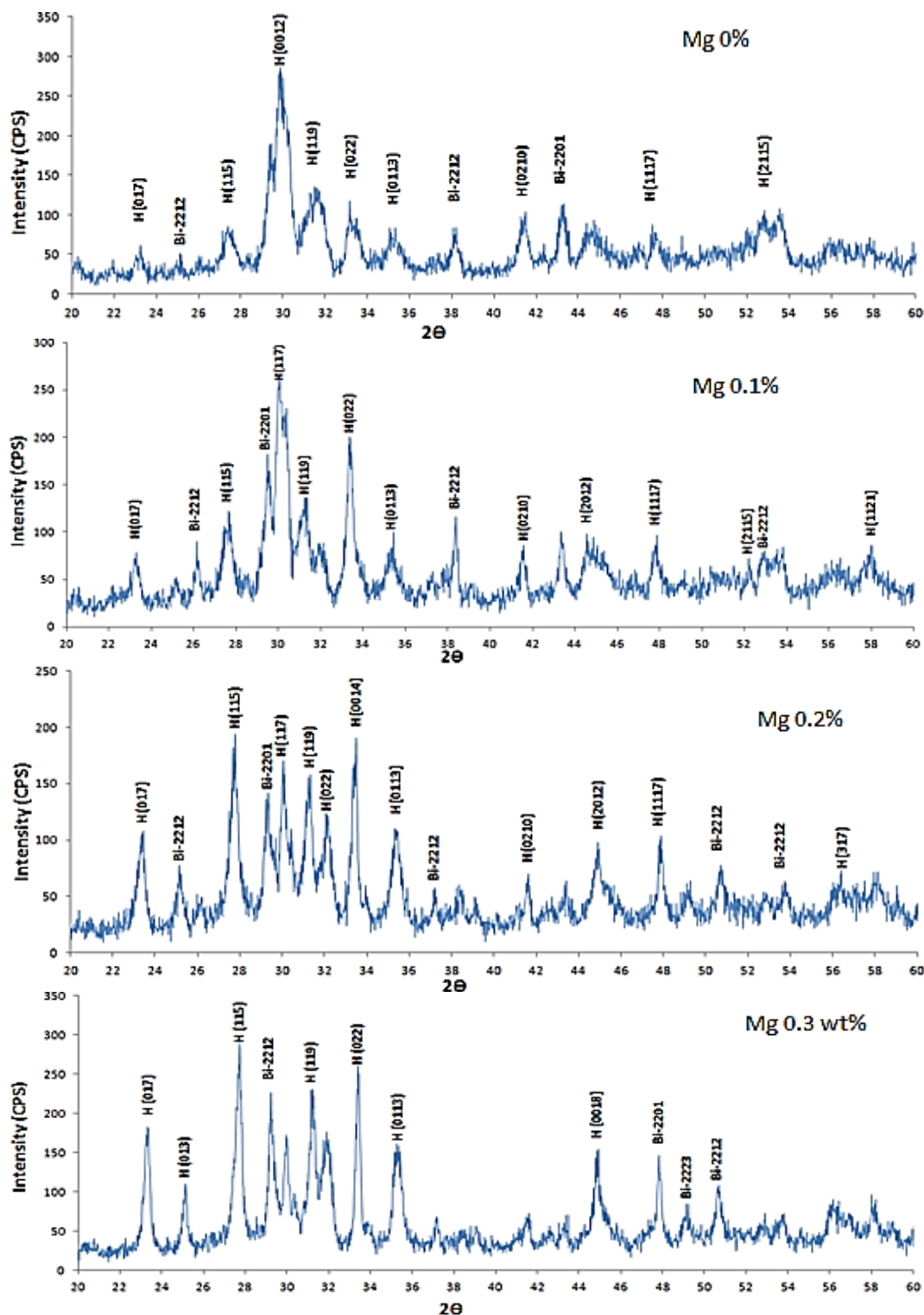


Fig. 1. XRD of  $\text{Bi}_{1.6}\text{Ag}_{0.4}\text{Sr}_{1.9}\text{Ba}_{0.1}\text{Ca}_2\text{Cu}_3\text{O}_{10+\delta}+(\text{MgO})_x$  where ( $x = 0.0, 0.1, 0.2, \& 0.3\text{wt}\%$ ).

The most intense pattern of the peak of samples belongs to a high- $T_C$  phase (Bi2223) that indicates as well that there is an increase in high- $T_C$  phase's volume fraction. All of the samples have shown improvement of the high  $T_C$  (Bi2223) peaks with the increase of the concentration of Mg, as it has been listed in Table1. This result has indicated that Addition by Mg results in improving the degree of the crystalline arrangements [29] and Bi-2223 phase's volume fraction, the stability and the formation of Bi2223 phase may be modified by adding elements with different

ionic radius and bonding properties. Grain size values of all of the samples have been estimated with the use of Deby Scherrer Formula, which has been represented below: [30]

$$L = \frac{0.9\lambda}{t \cos \theta}$$

$\lambda$  represents X-ray wave-length in nm, L represents crystalline size in nm, t represents FWHM (full width at half maximum) of maximum peak of intensity and  $\theta$  represents corresponding peak angle [30,31]. The sizes of the grain have been estimated from the patterns of the XRD and determined as 24.00, 21.44, 21.24, and 20.30 nm for sample Mg0, Mg0.1, Mg0.2, and Mg0.3, respectively. Results have been presented in Table1. Based on this table, the maximum grain size value has been found as 24nm for sample Mg0.

Table 1. Percentage volume fraction and grain size of Bi2223 phase and Bi2212 phase in  $\text{Bi}_{1.6}\text{Ag}_{0.4}\text{Sr}_{1.9}\text{Ba}_{0.1}\text{Ca}_2\text{Cu}_3\text{O}_{10+\delta}+(\text{MgO})_x$  ( $x = 0.0-0.3\text{wt}\%$ ) samples.

Sample wt%	Vol. fraction %		Grain size(nm)
	Bi-2223	Bi-2212	
MgO 0.0	77	23	24.00
MgO 0.1	78	22	21.44
MgO 0.2	79	21	21.24
MgO 0.3	80	20	20.23

Parameters (a, b, c), V, c/a and dm have been estimated as well from analysis of the XRD, as can be seen from the data in Table2. From estimating the lattice parameters (a, b, c), results have shown orthorhombic crystalline structure type for all of the samples. Changes in (c) axis may be a result of numerous causes, the first one was the increase in the concentration of the (O2), which has resulted from partially adding (MgO), such increase is taken by double (Bi-O) layers, causing stronger link due to a High (Mg) equivalence, which results in increasing the forces of the ion bonding that have been formed in (Bi-O) layers, thereby increasing lattice parameter c with increasing the content of Mg. It may be concluded that Bi2223 phase volume systematically varies with the c-parameter. Such variation in lattice parameters affects unit cell volume and then causes increased density. The second is that differences in ionic radius may result in causing deformities in lattice parameters [32]. Which is one of the driving forces to the pairing generation of the super-conductor holes that form bosons that have been considered as current carriers in the proposed super-conductor.

Table 2. Lattice parameters of  $\text{Bi}_{1.6}\text{Ag}_{0.4}\text{Sr}_{1.9}\text{Ba}_{0.1}\text{Ca}_2\text{Cu}_3\text{O}_{10+\delta}+(\text{MgO})_x$  ( $x = 0.0-0.3 \text{ wt}\%$ ) samples.

Specimens	x	a	b	c	$V(\text{Å}^3)$	dm	c/a
MgO 0.0	<b>0.0</b>	<b>5.4584</b>	<b>5.4458</b>	<b>37.741</b>	<b>1121.9</b>	<b>2.161781</b>	<b>6.9143</b>
MgO 0.1	<b>0.1</b>	<b>5.4596</b>	<b>5.4723</b>	<b>37.832</b>	<b>1130.3</b>	<b>2.095384</b>	<b>6.9295</b>
MgO 0.2	<b>0.2</b>	<b>5.4567</b>	<b>5.4501</b>	<b>37.886</b>	<b>1126.7</b>	<b>2.051626</b>	<b>6.9429</b>
MgO 0.3	<b>0.3</b>	<b>5.4598</b>	<b>5.4546</b>	<b>37.907</b>	<b>1128.9</b>	<b>1.997313</b>	<b>6.9430</b>

### 3.2. $T_c$ and Oxygen Content Results

Temperature dependence of electrical resistivity of  $\text{Bi}_{1.6}\text{Ag}_{0.4}\text{Sr}_{1.9}\text{Ba}_{0.1}\text{Ca}_2\text{Cu}_3\text{O}_{10+\delta}+(\text{MgO})_x$  ( $x = 0.0-0.3 \text{ wt}\%$ ) has been depicted in Figure2. It has been observed that samples showed metallic behavior, followed by super-conductivity transition with a transition temperature

that equals 138,139,140 and 141K for the composition with  $x= 0.0, 0.1, 0.2$  and  $0.3$  respectively. It is found from Table 3 that oxygen content ( $\delta$ ) of samples increases as the Mg content increases. Enhancing oxygen content ( $\delta$ ) results in the enhancement of hole concentration in Cu-O<sub>2</sub> layers, in addition to enhancement of critical temperature  $T_c$  from about 138K to 141K with increasing the content of Mg as can be seen from Figure 3. Which is an indication of the fact that increasing oxygen content ( $\delta$ ) and critical temperature  $T_c$  values has been a result of increasing the absorption of the oxygen throughout the superconductors' crystallization process. From results it may be concluded that oxygen content ( $\delta$ ) that equals 0.34910 represents the optimal value.

Table 3. Oxygen contents and critical temperatures ( $T_c$ ) of  $(Bi_{2-x}Ag_xSr_{1.9}Ba_{0.1}Ca_2Cu_3O_{10+\delta})$  with  $x= (0.10, 0.20, 0.30, 0.40)$ .

Specimen	$\delta$	$T_c$
MgO 0.00	<b>0.24835</b>	<b>138</b>
MgO 0.10	<b>0.2676</b>	<b>139</b>
MgO 0.20	<b>0.2859</b>	<b>140</b>
MgO 0.30	<b>0.3491</b>	<b>141</b>

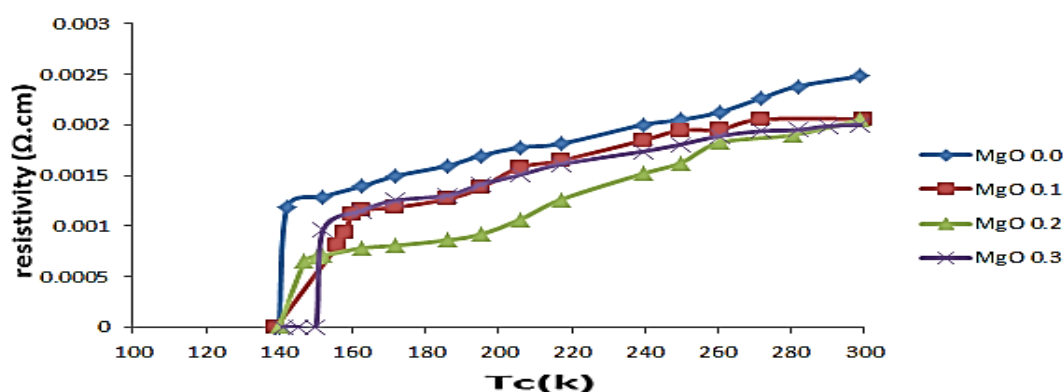


Fig. 2. The electric resistivity versus temperature behaviors of  $Bi_{1.6}Ag_{0.4}Sr_{1.9}Ba_{0.1}Ca_2Cu_3O_{10+\delta}+(MgO)_x$  ( $x = 0.0-0.3$  wt%).

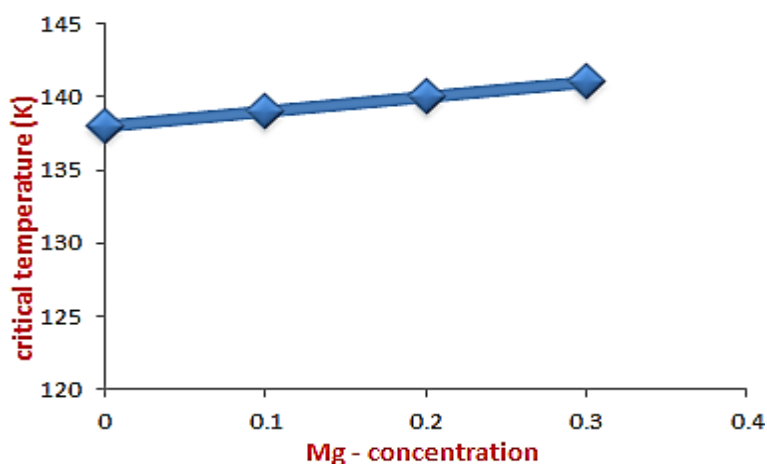


Fig. 4. Critical temperature as an (Mg) concentration function.

#### 4. Conclusions

In the present study, we investigated  $(\text{Bi}_{2-x}\text{Ag}_x\text{Sr}_{1.9}\text{Ba}_{0.1}\text{Ca}_2\text{Cu}_3\text{O}_{10+\delta})$ , super-conductor compounds for values of  $(x= 0.10, 0.20, 0.30 \text{ and } 0.40)$  that has been prepared with the use of the solid state reaction approach. The analyses of the XRD pattern had shown orthorhombic structures with high Bi-2223 super-conductor phase ratio, and, increase of c-axis lattice constant with an increase in the concentration of Ag. The optimal x value is that optimal ratio of substitution for the Ag in  $(\text{Bi}_{2-x}\text{Ag}_x\text{Sr}_{1.9}\text{Ba}_{0.1}\text{Ca}_2\text{Cu}_3\text{O}_{10+\delta})$ , compound is at  $x = 0.40$  where a high phase Bi2223 percentage appears. Substituting Ag in Ag in compounds of  $(\text{Bi}_{2-x}\text{Ag}_x\text{Sr}_{1.9}\text{Ba}_{0.1}\text{Ca}_2\text{Cu}_3\text{O}_{10+\delta})$ , had shown maximal value of  $T_c$  (138K) at  $x=0.40$ . moreover, oxygen content  $\delta$  were found to be increased by the increase of the concentration of Ag, since substitution produced of local pressure, hole carrier concentrations, variation electronic state and its distributions. AFM results have shown that surface roughness values and average diameter that samples have good homogeneous and crystalline surface and gave an optimal Nanosize value of 35nm at  $x=0.40$ .

#### References

- [1] B. Ozkurt, M.A Madre, A. Sotelo, E. Yakinci, B. Ozcelik, J. Supercond. Nov. Magn. 25, 799-804 (2012); <https://doi.org/10.1007/s10948-011-1346-7>
- [2] G. Yildirim, S. Bal, E. Yucel, M. Dogruer, M. Akdogan, A. Varilci, C. Terzioglu, J. Supercond. Nov. Magn. 25, 381-390 (2012); <https://doi.org/10.1007/s10948-011-1324-0>
- [3] B.Ozkurt, J. Mater. Sci. 24(11), 4233-4239 (2013); <https://doi.org/10.1007/s10854-013-1390-0>
- [4] A. Zelati, A. Amirabadizadeh, A. Kompany, H. Salamati, J.E. Sonier, J. Supercond. Nov. Magn. 27, 2185-2193 (2014); <https://doi.org/10.1007/s10948-014-2588-y>
- [5] H. Sozeri, N. Ghazanfari, H. Ozkan, A. Kilic, Supercond. Sci. Technol. 20, 522-528 (2007); <https://doi.org/10.1088/0953-2048/20/6/007>
- [6] A. Ghattas, M. Annabi, M. Zouaoui, F. Ben Azzouz, M. Ben Salem, Phys. C 468, 31-38 (2008); <https://doi.org/10.1016/j.physc.2007.10.006>
- [7] A. Ishii, T. Hatano, Phys. C 340, 173-177 (2000); [https://doi.org/10.1016/S0921-4534\(00\)00385-3](https://doi.org/10.1016/S0921-4534(00)00385-3)
- [8] E. Guilmeau, B. Andrzejewski, J.G. Noudem, Phys. C 387, 382 (2003); [https://doi.org/10.1016/S0921-4534\(02\)02360-2](https://doi.org/10.1016/S0921-4534(02)02360-2)
- [9] H. Baqiah, S.A. Halim, M.I. Adam, S.K. Chen, S.S.H. Ravandi, M.A.M. Faisal, M.M. Kamarulzama M. Hanif, Solid State Sci. Technol. 17, 81-88 (2009)
- [10] N.A.A. Yahya, R. Abd-Shukor, J. Supercond. Nov. Magn. 27, 329-335 (2014); <https://doi.org/10.1007/s10948-013-2302-5>
- [11] A. Ghattas, F. Ben Azzouz, M. Annabi, M. Zouaoui, M. Ben Salem, J. Phys. 97, 012175 (2008); <https://doi.org/10.1088/1742-6596/97/1/012175>
- [12] R. Mawassi, R. Awad, M. Roumie, M. Kork, I. Hassan, Adv. Mater. Res. 324, 241 (2011); <https://doi.org/10.4028/www.scientific.net/AMR.324.241>
- [13] A. Zelati, A. Amirabadizadeh, A. Kompany, H. Salamati, J. Sonier, J. Supercond. Nov. Magn. 27, 1369-1379 (2014); <https://doi.org/10.1007/s10948-013-2475-y>
- [14] S. Yavuz, O. Bilgili, K. Kocabas, J. Mater. Sci. 27, 4526-4533(2016); <https://doi.org/10.1007/s10854-016-4327-6>
- [15] W. Kong, R. Abd-Shukor, J. Supercond. Nov. Magn. 23, 257-263(2010)
- [16] M. Roumié, S. Marhaba, R. Awad, M. Kork, I. Hassan, R. Mawassi, J. Supercond. Nov. Magn. 27, 143-153 (2014); <https://doi.org/10.1007/s10948-013-2288-z>
- [17] M.A. Suazlinaa, S.Y.S. Yusaineea, H. Azhanb, R. Abd-Shukorc, R.M. Mustaqimd, Jurnal Teknologi 69(2), 49-52 (2014)
- [18] A. Zelati, A. Amirabadizadeh, A. Kompany, H. Salamati, J. Sonier, Indian J. Sci. Technol. 7, 123-134 (2014)

- [19] M. Zouaoui, A. Ghattas, M. Annabi, F. Ben Azzouz, M. Ben Salem, *Supercond. Sci. Technol.* 21, 125005 (2008); <https://doi.org/10.1088/0953-2048/21/12/125005>
- [20] S.F. Oboudi, M.Q. Mustafa, *Adv. Nanoparticles* 5, 75-82 (2016); <https://doi.org/10.4236/anp.2016.51009>
- [21] A. Zelati, *Indian J. Sci. Technol.* 6, 5552-5558 (2013)
- [22] M. Annabi, A. M'chirgui, F. Ben Azzouz, M. Zouaoui, M. Ben Salem, *Phys. C* 405, 25-33 (2004); <https://doi.org/10.1016/j.physc.2004.01.012>
- [23] Z.Y. Jia, H. Tang, Z.Q. Yang, Y.T. Xing, Y.Z. Wang, G.W. Qiao, *Phys. C* 337, 130-132 (2000); [https://doi.org/10.1016/S0921-4534\(00\)00072-1](https://doi.org/10.1016/S0921-4534(00)00072-1)
- [24] O. Bilgili, K. Kocabas, *J. Mater. Sci.* 25, 2889-2897 (2014); <https://doi.org/10.1007/s10854-014-1956-5>
- [25] K. Kocabas, O. Ozkan, O. Bilgili, Y. Kadioglu, H. Yilmaz, *J. Supercond. Nov. Magn.* 23, 1485-1492 (2010); <https://doi.org/10.1007/s10948-010-0800-2>
- [26] Noor S. Abed<sup>1</sup>, Abdulsalam S. Baqi<sup>1</sup>, Bilal A. Omer<sup>2</sup>, Shatha H. Mahdi<sup>3</sup>, Kareem A. Jaseem<sup>3</sup> and Saja Amer Ahmed<sup>3</sup> Manufacturing and studying the effect of partial substitution on the properties of the compound  $\text{Bi}_{2-x}\text{Ag}_x\text{Sr}_{1.9}\text{Ba}_{0.1}\text{Ca}_2\text{Cu}_3\text{O}_{10+\delta}$  superconductors. *Journal of Physics: Conference Series*, Volume 1178, International Workshop in Physics Applications 20-21 November 2018, Fallujah, Anbar, Iraq; <https://doi.org/10.1088/1742-6596/1178/1/012025>
- [27] Bilal A. Omar, Sabah J. Fathi, Kareem A. Jassim, "Effect of Zn on the Structural and Electrical Properties of High Temperature  $\text{HgBa}_2\text{Ca}_2\text{Co}_3\text{O}_{8+\delta}$  Superconductor", *Technologies and Materials for Renewable Energy, Environment and Sustainability*, vol.1968pp: 030047-1-030047-9,(2018)..
- [28] A. Younis, N. A. Khan and N. U. Bajwa, "Dielectric Properties of  $\text{Cu}_{0.5}\text{Tl}_{0.5}\text{Ba}_2\text{Ca}_3\text{Cu}_{4-y}\text{Zn}_y\text{O}_{12-\delta}$  ( $y = 0, 3$ ) Superconductors" *Journal of the Korean Physical Society*, vol.57,no.6,pp. 1437-1443, 2010; <https://doi.org/10.3938/jkps.57.1437>
- [29] M. Mumtaz, N.A. Khan and S. Khan "Frequency dependent dielectric properties of  $\text{Cu}_{0.5}\text{Tl}_{0.5}\text{Ba}_2\text{Ca}_2(\text{Cu}_{3-y}\text{My})\text{O}_{10-\delta}$  superconductor" *J. Appl. Phys.* vol.111, issue 3,pp.013920-1-10,2012; <https://doi.org/10.1063/1.3673307>
- [30] Bilal Ahmed Omar, Rabab Shakour Ali "A Study of Substitution the Element of (La<sup>+3</sup>) on the Structural and Electrical Properties of the Compound Ferrite ( $\text{Co}_{0.25}\text{Ni}_{0.25}\text{Zn}_{0.5}\text{La}_x\text{Fe}_{2-x}\text{O}_4$ )" *NeuroQuantology*, March 2021, Volume 19, Issue 3, Page 56-61, (2021); <https://doi.org/10.14704/nq.2021.19.3.NQ21028>
- [31] E. Guilmeau a,\*, B. Andrzejewski a,b, J.G. Noudem The effect of MgO addition on the formation and the superconducting properties of the  $\text{Bi}_2\text{Tl}_2\text{O}_8$  phase *Physica C* 387 (2003) 382-390; [https://doi.org/10.1016/S0921-4534\(02\)02360-2](https://doi.org/10.1016/S0921-4534(02)02360-2)
- [32] Thabit.H.A.;Hermiz.G.Y and Al-jurani.B.A (Superconducting properties of the  $(\text{Bi}_{0.8}\text{Pb}_{0.2})_2(\text{Sr}_{0.9}\text{Ba}_{0.1})_2\text{Ca}_2\text{Cu}_{3-x}\text{Ni}_x\text{O}_{10+\delta}$  system, *Baghdad Science Journal*, vol.8 (2),607,2011; <https://doi.org/10.21123/bsj.8.2.607-612>